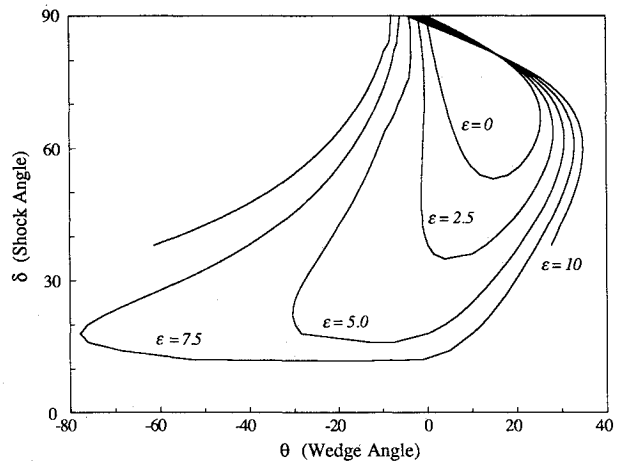

Fig. 3 Variations of shock angle and wedge angle, $M_f = 6$, $\bar{Q} = 20$, equilibrium chemistry, $\epsilon = 0, 2.5, 5, 7.5, 10$.

With the shocked state determined, the velocity can be resolved into components normal and parallel to the reaction front and formulas similar to Eqs. (4–6) applied again, now with Q nonvanishing. In this case there are two roots. When $\epsilon = 0$, this procedure recovers the results of the single-front calculation.

Figure 3 is typical of the results obtained in this way. Curves that terminate do so at points where the shocked flow is parallel to the reactive front ($\alpha = 0$). Note that negative wedge angles are formally possible but seem unlikely to have physical significance.

These results are of interest in the context of the calculations of Fujiwara et al. for they show that increases in ϵ lead to a commensurate increase in the final refraction angle. Specifically, $\epsilon = 6$ deg increases the maximum deflection by about 6 deg so that a wedge angle of 30 deg is possible. Since the numerical results for $\bar{Q} = 20$, $M_f = 6$ reveal a value of ϵ of about 10 deg (see Fig. 5 of Ref. 3), there is no contradiction between the numerical results and the necessary conditions defined by the Rankine-Hugoniot conditions.

Conclusions

Some of the numerical results for oblique detonations obtained by Fujiwara et al. are not consistent with limits defined by single-front Rankine-Hugoniot conditions. However, when two-dimensional effects are accounted for in an approximate fashion using a dual-front model, the inconsistency is eliminated.

Acknowledgment

This work was supported by the Air Force Office of Scientific Research. We are grateful to J. Powers for several helpful discussions.

References

[1]Gross, R. A., "Oblique Detonation Waves," *AIAA Journal,* Vol. 1, No. 5, 1963, pp. 1225–1227.

[2]Hertzberg, A., Bruckner, A. P., and Bogdonoff, D. W., "The Ram Accelerator: A New Chemical Method of Achieving Ultrahigh Velocities," 37th Meeting of the Aeroballistic Range Association, Quebec, Canada, Sept. 1986.

[3]Fujiwara, T., Matsuo, A., and Nomoto, H., "A Two-Dimensional Detonation Supported by a Blunt Body or Wedge," AIAA Paper 88-0098, Jan. 1988.

[4]Landau, L. D., and Lifshitz, E. M., *Fluid Mechanics,* Pergamon Press, New York, 1959.

[5]Buckmaster, J., and Ludford, G. S. S., "The Effect of Structure on the Stability of Detonations. I. Role of the Induction Zone," *Proceedings of the 21st Symposium (International) on Combustion.* The Combustion Institute, Pittsburgh, 1986, pp. 1669–1676.

Accuracy of Upwind Schemes Applied to the Navier-Stokes Equations

E. von Lavante*
Old Dominion University, Norfolk, Virginia

Introduction

UPWIND schemes for solving the compressible Euler and Navier-Stokes equations have been known for almost 30 years, but they have been applied to predictions of flows about complex geometries only relatively recently.

The Euler solvers based on the van Leer flux-vector splitting[1,3,6] are generally capable of accurate and reliable predictions of two- and three-dimensional flows. They have been extended to the Navier-Stokes equations by, among others, Thomas and Walters,[2] with mixed results. On grids with sufficiently high resolution, the results were generally good. However, on coarser grids and grids with significant stretching, the boundary layers were badly diffused. It has been shown recently by Hänel et al.[3] that some of this excessive diffusion is because of the application of flux limiters and formulations that are formally of lower order accuracy than the third-order upwind-biased MUSCL procedures.[2] Van Leer et al.[1] point out that the van Leer flux-vector splitting in its finite-volume form is actually neglecting the interaction of linear waves at cell interfaces and, therefore, solves the corresponding Riemann problem only approximately. A more accurate solution to the Riemann problem at the cell interfaces (interface between two states) as proposed by, for example, Roe,[4] will reduce the effect of artificial dissipation. This has been demonstrated conclusively in Ref. 1 for a few hypersonic cases. However, based on these few cases, it is still difficult to make a general statement.

The purpose of this Note is to present the results of a systematic comparison of the different forms of the van Leer flux-vector splitting with Roe's flux-difference splitting as applied to a simple viscous configuration. Attention is paid to the effects of spacial accuracy, grid resolution, and grid stretching on the accuracy of the resulting flowfield.

Approach

The comparison of the different schemes was carried out for a flat plate at a freestream Mach number $M_\infty = 0.5$ and reference Reynolds number $Re_o = 5 \times 10^3$. A rectangular grid with uniform spacing along the plate and various degrees of stretching in the normal direction extended two unit lengths downstream and three unit lengths (10 boundary-layer thicknesses at the outflow) in the direction normal to the plate. The main goal of the present work was the determination of the accuracy of the different schemes as a function of the various rates of stretching of the grid in the normal direction; therefore, the usual grid refinement study was performed for constant grid stretching. Since a simple geometric grid distribution was taken in the normal direction, the stretching factor f was constant throughout the grid and was defined as the ratio of two spacings in the y direction (normal to the plate), $f = (\Delta y_i / \Delta y_{j-1})$. Three rates of stretching were selected for this study:

Received Feb. 8, 1988; revision received May 22, 1989.

*Associate Professor, Mechanical Engineering and Mechanics Department.

Table 1 Grid dimensions, number of points in the boundary layer.

$f = 1.3$	$f = 1.1$	$f = 1.05$
33 × 17, 8	33 × 34, 9	33 × 51, 10
33 × 20, 10	33 × 41, 12	33 × 64, 14
33 × 23, 12	33 × 48, 16	33 × 78, 20
33 × 25, 15	33 × 55, 22	33 × 92, 27

$f = 1.3$ (high), $f = 1.1$ (medium), and $f = 1.05$ (small). For each f and each scheme, the grid refinement was carried out in the physical domain by subsequently halving the grid spacing in the normal direction only, resulting in the following sequence of the first grid spacing Δy_1 (next to the solid wall): 0.015, 0.0075, 0.00375, and 0.001875. The entire matrix of the grid combinations and the corresponding number of grid points, as well as the number of points in the boundary layer, are shown in Table 1. In the x direction along the plate, 33 points were uniformly distributed. This distribution was the same for all of the cases.

Presently, the number of the possible upwind schemes and their variations seems to be endless. In order to keep the extent of this study within manageable limits, only two main representatives of the upwind schemes, with some of the possible modifications, were considered here. The schemes were presented in sufficient detail in previous publications and will, therefore, be mentioned here only briefly.

Scheme I

—An implicit flux-vector splitting scheme (FVSS) for solving the Navier-Stokes equations, as introduced by von Lavante and Melson.[5] This finite-volume scheme is based on van Leer splitting and uses the MUSCL approach to determine the value of the dependent conservative variables Q at the cell faces. No flux limiters were applied because of the low freestream Mach number. Three versions of this method were investigated: 1) second-order scheme with extrapolation of Q in the computational (transformed) domain; 2) second-order scheme with extrapolation of Q in the physical domain, taking into account the unequal length of the cells; and 3) third-order scheme with extrapolation of Q in the computational domain. All of the schemes use the second-order viscous terms and are, therefore, formally second-order accurate. The preceding notation relates only to the convective terms.

Scheme II

—An implicit flux-difference splitting scheme (FDSS), based on Roe's approximate Riemann solver[4] in its finite-volume form. It again employed the MUSCL differencing without flux limiters. The formulation uses the well-known Roe averaging[4] to approximately solve the Riemann problem at the cell interfaces. Two versions of this method were treated: 1) third-order form of the basic scheme and 2) third-order form with explicitly added artificial dissipation. This version of the FDSS seems to negate the main advantages of this scheme. It has been proposed as a "quick fix" for some of the problems this scheme experienced at stagnation points of hypersonic and high Mach number supersonic flows. Here, in the expression for the numerical flux at a cell interface $\tilde{F}$ is[1]

$$\tilde{F} = \tfrac{1}{2}\,[F_R + F_L - \hat{S}|\hat{\Lambda}|\hat{S}^{-1}(Q_R - Q_L)] \qquad (1)$$

where the subscripts R and L denote the "right" and "left" states relative to a quasi-one-dimensional cell interface and F_L and F_R are the physical fluxes formed from the corresponding conservative variables Q_L and Q_R. The diagonal matrix $|\hat{\Lambda}|$ is modified by additional damping terms. The new diagonal matrix $|\hat{\Lambda}|_\epsilon$ (the caret denotes expression formed from Roe's averaged variables) is obtained from $|\hat{\Lambda}_i|_\epsilon = d_i$, where $d_i = |\hat{\Lambda}_i|$ when $|\hat{\lambda}_i| \geq \epsilon$ and $d_i = 1/2\epsilon\,[(\hat{\lambda}_i)^2 + \epsilon^2]$ when $|\hat{\lambda}_i| < \epsilon$. The value of the damping coefficient was $\epsilon = 0.2$. This seems to be at the higher end of the recommended range. The results obtained from this version should be representative for this approach. The boundary conditions used in this study are given in Ref. 5.

A meaningful comparison of the results requires proper choice of a measure of the global error. Many investigators used, for this purpose, the skin-friction coefficient C_f. However, very early in the present investigation it was found that the C_f coefficient was not an appropriate measure of the global accuracy. In many cases, the C_f values showed very good agreement with the theoretical value given by the Blasius solution since the slope of the velocity profile at the wall was correct, but the velocity profile significantly deviated from the Blasius profile in the area of high second derivative of the velocity ("knee" of the velocity profile), as shown in Fig. 1. Therefore, it was decided to use an rms of the difference between the present velocity results and the Blasius results within the boundary layer

$$E_{rr} = \sqrt{\frac{1}{n}\sum_{k=1}^{n}(u_k - u_{\text{Blasius}})^2} \qquad (2)$$

where the Blasius results were modified to account for compressibility.

The error E_{rr} was evaluated in the middle of the flat plate in order to limit the influence of the plate leading edge as well as that of the nonreflection outflow boundary conditions.

It should be noted that the Blasius solution is the result of a different (simplified) mathematical model of the flow than the more general Navier-Stokes equations solved in the present study. The present solution will tend to a slightly different result as $\Delta y \to 0$, so that $\Delta y \to 0$, $E_{rr} \to$ const, and not, as was expected, $E_{rr} \to 0$. This is particularly noticeable in the case of the very fine grids.

Results

The resulting grid refinement plots, showing the $\log_{10}(E_{rr})$ as a function of the $\log_{10}$ of the first (smallest) grid spacing in the normal direction Δy_1, indicated that the second-order FVSS was very similar for the extrapolations in the physical and the computational domains. The highest grid stretching reduced the accuracy of the method to less than first order. As the stretching was reduced, the accuracy improved, approaching the formal second-order level. The third-order FVSS has the same general tendency, with somewhat lower error levels than the second-order schemes. In the case of $f = 1.05$ (lowest stretching), second-order accuracy is recovered on the coarser grids and on the finest grids; the error approaches the final constant value.

In contrast to the FVSS, the accuracy of the FDSS is independent of the stretching. Even on the highly stretched coarse grid, with $f = 1.3$, the scheme is second-order accurate. The quality of these results becomes evident when the boundary-

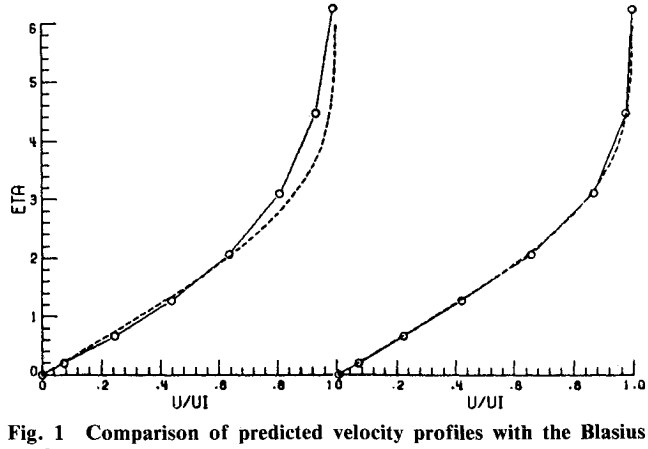

Fig. 1 Comparison of predicted velocity profiles with the Blasius results.

layer u-velocity profiles from the FVSS and FDSS are compared. The results shown in Fig. 1 were obtained on the coarsest grid (33×17) with the highest stretching. The result from the FDSS is clearly superior to the FVSS.

Finally, the addition of artificial damping effectively negates the advantage of the FDSS, making its results comparable with the FVSS.

The preceding behavior is explained by detailed examination of the artificial damping terms. Extending the approach of Vatsa et al.[6] the damping term in Eq. (1) is written in the j direction normal to the plate

$$D_{i,j+\frac{1}{2}} = \frac{1}{2}\tilde{T}\begin{bmatrix} |\tilde{\lambda}_1| & \Delta s \\ |\tilde{\lambda}_2| & \tilde{\rho}\Delta U_\eta \\ |\tilde{\lambda}_3|\tilde{\rho}\Delta J^+/2\tilde{c} \\ |\tilde{\lambda}_4|\tilde{\rho}\Delta J^-/2\tilde{c} \end{bmatrix} y_\eta = y_\eta D' \tag{3}$$

where Δs is the difference in entropy between the left and right states, ΔU_η is the jump in normal velocity, and ΔJ^+, ΔJ^- the jumps in the corresponding Riemann invariants at the cell face $i, j+\frac{1}{2}$. It has been shown in Ref. 6 that D' is small in a boundary layer, since $\tilde{\lambda}_1$, $\tilde{\lambda}_2 = \tilde{v}$ are small and multiply Δs and $\tilde{\rho}\Delta U_\eta$, which are 0(1); ΔJ^+ and ΔJ^- are also small. The resulting contribution of the damping to the flux difference is

$$\delta D_j = D_{i,j+1/2} - D_{i,j-1/2} = \delta(y_\eta D')_j \tag{4}$$

which is clearly proportional to the grid stretching $y_{\eta\eta}$ in the direction normal to the wall. Since D' is small, the effect of grid stretching on the results will also be small.

In the case of the flux-vector splitting and the central-difference schemes, expressions similar to Eq. (3) can be obtained.[6] Here, however, the damping term D' is not small, since $\tilde{\lambda}_1$ and $\tilde{\lambda}_2$ are not small.[6] The grid stretching in Eq. (4) will, therefore, increase the artificial damping of the scheme and thus contaminate the results in viscous sublayers. The addition of small damping ϵ to $|\tilde{\lambda}_i|$ in the Roe's scheme had the same effect and resulted in errors that were similar to the flux-vector splitting scheme.

Conclusions

The present comparative study of the different upwind schemes for solving the Navier-Stokes equations, as applied to a simple problem, indicates that the flux-difference splitting scheme produces more accurate results on coarse, highly stretched grids than the flux-vector splitting scheme.

Acknowledgment

This work was supported by NASA Langley Research Center Grant NAG-1-633.

References

[1]van Leer, B., Thomas, J. L., Roe, P. L., and Newsome, R. W., "A Comparison of Numerical Flux Formulas for the Euler and Navier-Stokes Equations," AIAA Paper 87-1104, June 1987.

[2]Thomas, J. L. and Walters, R. W., "Upwind Relaxation Algorithm for the Navier-Stokes Equations," AIAA Paper 85-1501, July 1985.

[3]Hänel, D., Schwane, R., and Seider, G., "On the Accuracy of Upwind Schemes for the Solution of the Navier-Stokes Equations," AIAA Paper 87-1105, June 1987.

[4]Roe, P. L., "Approximate Riemann Solvers, Parameter Vectors, and Difference Schemes," *Journal of Computational Physics*, Vol. 43, Feb. 1981, pp. 357-372.

[5]von Lavante, E. and Melson, N. D., "Simple Numerical Method for Predicting Steady Compressible Flows," AIAA Paper 87-2409, Aug. 1987.

[6]Vatsa, V., Thomas, J. L., and Wedan, B., "Navier-Stokes Computations of Prolate Spheroids at Angle of Attack," AIAA Paper 87-2627, Aug. 1987.

Structure of the Contact Discontinuity of Nonstationary Mach Reflections

Gabi Ben-Dor*
Ben-Gurion University of the Negev, Beer Sheva, Israel

THE structure of the contact discontinuity at the triple point of a pseudosteady Mach reflection was reconsidered, as it is known that in some cases the classical "three shock theory" fails to accurately predict the angles between the four discontinuities of the triple point.[1] Based on experimental records, the slipstream was replaced by an angular mixing zone. Integrating this change into the "three shock theory" resulted in very good agreement with the experimental records.

Introduction and Theoretical Background

When a planar shock wave encounters a sharp compressive corner, such as a leading edge of a wedge, in a shock tube, two different types of reflection can occur. They are regular reflection and Mach reflection. The type of reflection which occurs depends for a given gas on the incident shock wave Mach number M_i and the reflecting wedge angle θ_w.

The Mach reflection consists of four discontinuities, the incident shock i, the reflected shock r, the Mach stem m, and the slipstream s. These four discontinuities coincide at the triple point T. Over a plane wedge, the triple point moves along a straight line making an angle X with the reflecting wedge surface. The shock reflection process over plane wedges in shock tubes was found to be self-similar by many experimentalists.[2-5]

By attaching a frame of reference to the triple point, the nonstationary Mach reflection is transformed to a pseudosteady Mach reflection (Fig. 1a). Thus, the shock waves can be treated using the steady flow theory. Assuming that at the vicinity of the triple point the shock waves are straight, the oblique-shock-wave-conservation equations can be applied separately to the shock waves. The conservation equations are

$$\rho_i u_i \sin\phi_j = \rho_j u_j \sin(\phi_j - \theta_j) \tag{1}$$

$$\rho_i \tan\phi_j = \rho_j \tan(\phi_j - \theta_j) \tag{2}$$

$$P_i + \rho_i u_i^2 \sin^2\phi_j = P_j + \rho_j u_j^2 \sin(\phi_j - \theta_j) \tag{3}$$

$$h_i + 1/2 u_i^2 \sin^2\phi_j = h_j + 1/2 u_j^2 \sin^2(\phi_j - \theta_j) \tag{4}$$

where ρ is the density, P the static pressure, h the enthalpy, u the flow velocity, ϕ the incident angle, and θ the deflection angle, $i=0$ and $j=1$ for the incident shock, $i=1$ and $j=2$ for the reflected shock, and $i=0$ and $j=3$ for the Mach stem. If the flow regions are assumed to be in thermodynamic equilibrium, then the above set of 12 equations consists of 18 variables, namely, P_0, P_2, P_3, T_0, T_1, T_2, T_3, u_0, u_1, u_2, u_3, ϕ_1, ϕ_2, ϕ_3, θ_1, θ_2, and θ_3. Usually four of these 18 variables, namely, P_0, T_0, u_0, and ϕ_1 are known as initial conditions. Thus, the above set of 12 equations contains 14 unknowns.

Received Feb. 13, 1989; revision received July 24, 1989.

*Professor, Department of Mechanical Engineering, Pearlstone Center for Aeronautical Engineering.